Catalysis Surveys from Asia (2024) 28:36–47
https://doi.org/10.1007/s10563-023-09410-1

ORIGINAL ARTICLE

Synthesis of *n*-Butyl Levulinate Over Caesium Containing Heteropoly Acid Supported Zeolite β Catalysts

Kalpana Maheria[1,2] · Ramesh Kumar Chowdari[2,3] · Janusz Kozinski[4] · Ajay Kumar Dalai[2]

Received: 21 May 2023 / Accepted: 30 September 2023 / Published online: 6 November 2023

Abstract

The aim of the present work is to investigate an environmentally benign method for the catalytic conversion of biomass derived compounds into fine chemicals. Levulinic acid (LA) is one of the key biomass-derived chemicals that can be converted into biofuels and various other value-added chemicals. *n* -Butyl levulinate ester is an important chemical used in the production of fuel additives, solvents, plasticizing agents, and odorous substances. The work presented here focused on the esterification of *n*-butyl levulinate by reaction of LA and *n*-butanol in the presence of synthesized 20% tungstophosphoric acid (TPA) supported zeolite β (TPA-Zβ), CsTPA-Zβ and Cs-Zβ catalysts. Various catalyst characterization techniques have been used, specifically, XRD, SEM–EDS, FT-IR, nitrogen physisorption and NH_3 -TPD. The highest % yield of *n* -butyl levulinate is obtained with shorter reaction time in the case of a 20% TPA supported zeolite β catalyst, calcined at 300 °C. The addition of Cs ions to TPA appears to improve catalytic performance.

Graphical Abstract

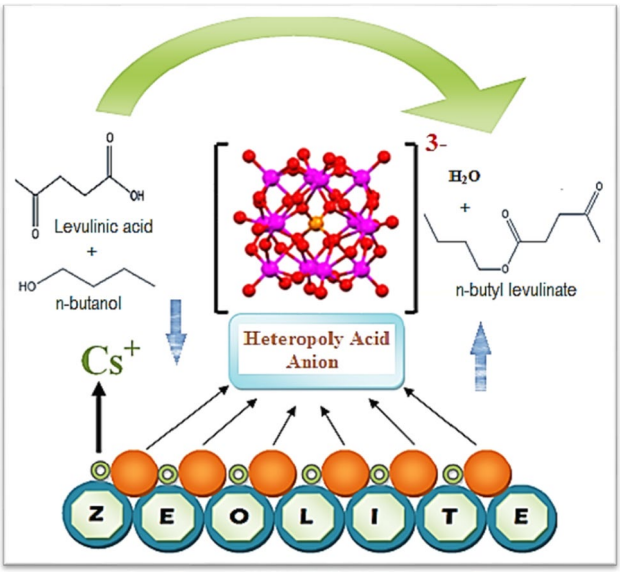

Keywords Supported solid acid catalyst · Zeolite · Cs salt of heteropoly acid · Levulinic acid · *n*-Butyl levulinate

Extended author information available on the last page of the article

1 Introduction

There is a growing interest in the development of environmentally benign methods for the conversion of biomass-based derivatives into fine chemicals and valeric biofuels to control industrial pollution. Levulinic acid (LA) is one of the most important chemicals that can be derived from lignocellulose, a low cost and widely available carbon source. As reported by the Department of Energy, United States, LA is a promising building block for chemistry in 2004 and again in 2010 [1]. Its use for the production of industrially valuable chemicals is of great current research interest. Levulinic esters are one of the significant derivatives of LA and are obtained by the esterification reaction of LA in the presence of a suitable acid catalyst, such as sulphuric, polyphosphoric or *p*-toluenesulfonic acid in a homogeneous medium [2, 3]. However, heterogeneous catalysts, are preferable over the homogeneous ones due to their notable merits in terms of easy separation, regeneration, pollution abatement due to non-corrosive nature and lack of hazardous waste generation. Very few reports are available on the esterification reaction of LA with *n*-butanol to produce *n*-butyl levulinate using heterogeneous catalysts [2, 4–7].

Zeolites are a class of crystalline nanoporous solids that are extensively used as solid acids. In addition, their regular and uniform pores provide highly shape-selective properties that control selective product formation [8]. Zeolite beta (Zβ), one among the over 260 unique zeolitic structures produced, is a large pore size zeolite. It contains an interconnected three-dimensional (*3D*) channel system with 12-membered ring openings with an average diameter of 0.67 nm. This zeolite has gained much interest in the last two decades. Zeolite H-Zβ is a crystalline solid containing more than one polymorph within the structure, resulting in crystallographic defects, and possesses unique acidic properties [9, 10]. The large pore openings and high surface area of H-Zβ zeolite make it a very promising solid acid catalyst for several shape-selective organic transformations which are of significant interest for industrial applications in the area of fine chemical synthesis, petroleum chemistry, refining processes, etc. [11].

Heteropoly acid (HPA) compounds are an established non-corrosive acid catalysts with high acidic properties in homogeneous and heterogeneous catalysis [12]. HPAs are also known for their Brønsted acidity (presence of hydrated and non-hydrated protons), particularly, a 12-tungstophosphoric acid (TPA), which belongs to the HPA family and exhibits super acidity and relatively high thermal stability compared to other HPA systems**.** The origin of the strong acidity of HPAs is shown in Fig. 1 [13–17].

Specifically, the catalytic activity of heteropoly acids in an organic solvent is much higher compared to mineral acids like sulfuric acid [16, 18, 19]. The salient features shown in Fig. 1 makes them a good catalyst to perform reactions through a mild chemical ('Chemie Douce') approach. Furthermore, the other advantage of heteropoly acid is that minimal or no side reactions occur. Specifically, nitration,

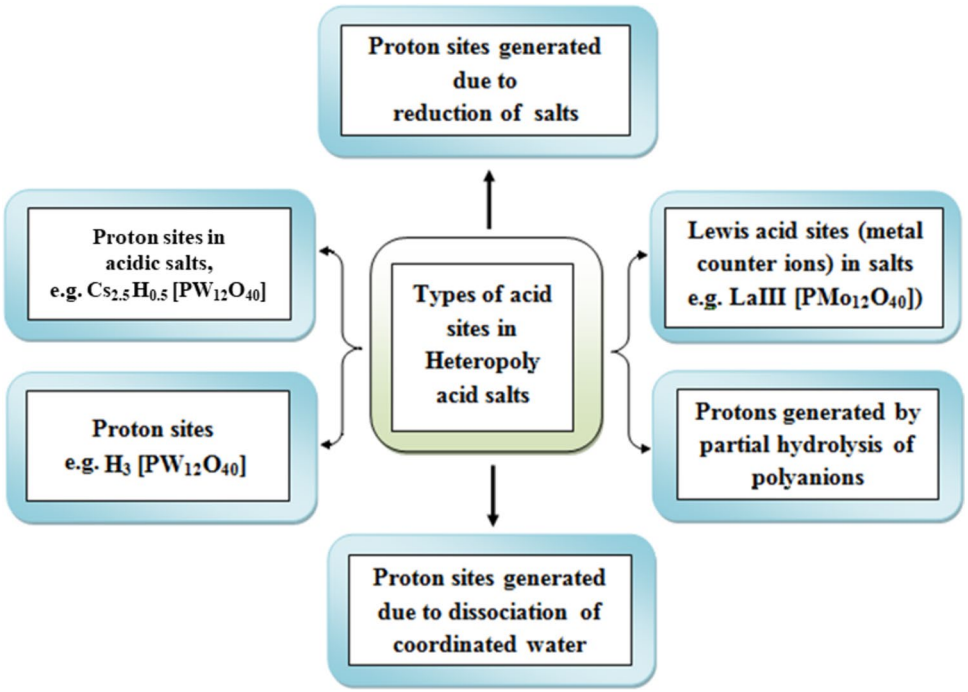

Fig. 1 Origin of strong acidity of heteropoly acids

sulfonation or chlorination, which are common issues with mineral acids [18, 19].

The Keggin structure of TPA possesses a central PO_4 tetrahedron, connected to twelve WO_6 octahedra (Fig. 2). The overall -3 charge of heteropoly anion needs cations (mono/polyvalent) for electroneutrality. The neutralization of this negative charge with three protons (H^+) leads to generation of Brønsted acidity [12]. However, these solid acids, in general, possess a low surface area, low thermal stability, porosity and high solubility in polar solvents [12]. To circumvent these drawbacks, HPAs are supported by entrapping the TPA salt on a support matrix, for example, on titania, zirconia, mesoporous silica etc. Supported heteropoly acid salts possess more surface acidic sites as compared to their bulk analogues and are proven efficient catalysts for several organic transformations [20, 21]. Zeolites with well-defined pores are also used as support system for TPA, and several shape-selective catalysts have been reported popularly referred as intrazeolite heteropoly acids [22]. For example, incorporation of 12-phosphomolybdic acid into the super cages of Y-type zeolite, employing "ship-in-a-bottle" synthesis method, was found to be a good catalyst for liquid phase reactions [22]. Similarly, using sol–gel methods, Keggin-type HPAs were incorporated into a silica matrix and tested for Friedel–Crafts alkylation reactions. The nature of counter ion is a key parameter that affects acidity, thermal stability, porosity and solubility to a large extent. HPAs act as acid catalysts due to the lower charge density on the surface of the HPA molecule, for example, $H_3PW_{12}O_{40}$ and $H_3PMo_{12}O_{40}$ resulting in no charge localization, making the protons mobile, resulting in strong Brønsted acidity. Salts containing small cations become readily soluble in an aqueous medium and have a lower surface area than the salts of large monovalent cations such as K^+, NH_4^+, Cs^+, etc. Literature reveals that the Cs^+ salt, $Cs_{2.5}H_{0.5}$ $[PW_{12}O_{40}]$ exhibits high hydrophobicity and high surface area (compared to pure HPA salts), in the range of 100–200 m^2g^{-1} and is known to be an efficient solid acid catalyst for numerous organic transformations [16].

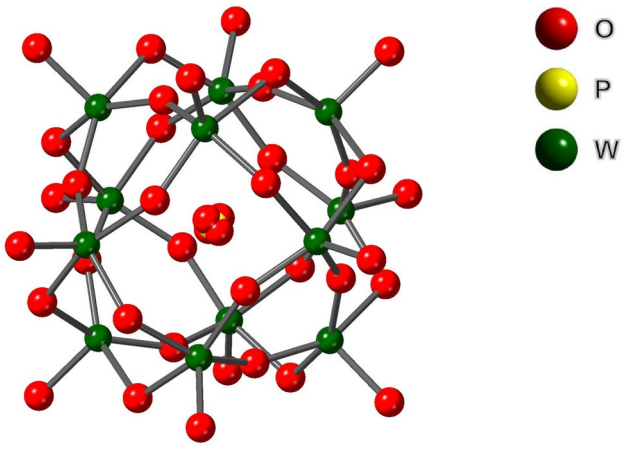

Fig. 2 Molecular image of Keggin structure showing a location of elements in the Heteropoly tungstate crystal

Here, an attempt has been made for the synthesis of *n*-butyl levulinate from LA and *n*-butanol by combining the properties of TPA and H-Zβ, by supporting TPA/CsTPA on zeolite β (H-Zβ) catalysts via an esterification reaction. The resultant catalyst is environmentally friendly because HPA and zeolites are non-corrosive, easily separable, reusable, and the acidity of this catalyst falls within the range of superacid. Bokade et al. have used supported dodecatungsto phosphoric acid (DTPA) on acid-treated clay for LA esterification [23]. To the best of the authors' knowledge, there are no studies reported on LA esterification using caesium exchanged heteropoly acid supported zeolite H-Zβ (Zβ) catalyst to obtain *n*-butyl levulinate. In the present study, we also attempted to synthesize *n*-butyl levulinate from levulinic acid (LA) and *n*-butanol using various catalysts [20% TPA supported zeolite β (TPA-Zβ), 20% Cs exchanged TPA supported on Zβ (CsTPA-Zβ) and 20% Cs supported zeolite β 20% (Cs-Zβ)] via esterification reaction (Scheme 1).

The synthesized catalysts are characterized by various techniques such as X-ray diffraction (XRD), N_2 sorption isotherm analysis to determine the surface area, ammonia temperature program desorption (NH_3-TPD) analysis to measure the acidity, Fourier transform infrared spectroscopic (FT-IR and ATR-FTIR) analysis to confirm functional groups present in the materials, etc.

2 Experimental Section

2.1 Materials and Methods

The zeolites H-Beta [Zβ; Si/Al = 25] was received from Sud-Chemie India Pvt Ltd., Vadodara, Gujarat, INDIA. Levulinic acid, *n*-butanol, Caesium carbonate and 12-tungsto phosphate hydrate were obtained from Alfa Aesar, USA. All the reagents were of analytical grade and used without further purification. The solvents were distilled before use.

2.1.1 Catalyst Preparation

The Cs salt of 12-TPA supported on zeolite H-Zβ catalyst was prepared by a two-step impregnation method. Initially zeolite β was impregnated with the Cs precursor, followed by TPA with nominal Cs:TPA ratio of 2:1 to obtain $Cs_2H[PW_{12}O_{40}]$ in the final catalyst. In a typical procedure, the calculated amount of $CsCO_3$ is dissolved in distilled water, added to the Zβ and suspended in distilled water with vigorous stirring. The required amount of aq. TPA solution was added dropwise to obtain a Cs salt of TPA equivalent

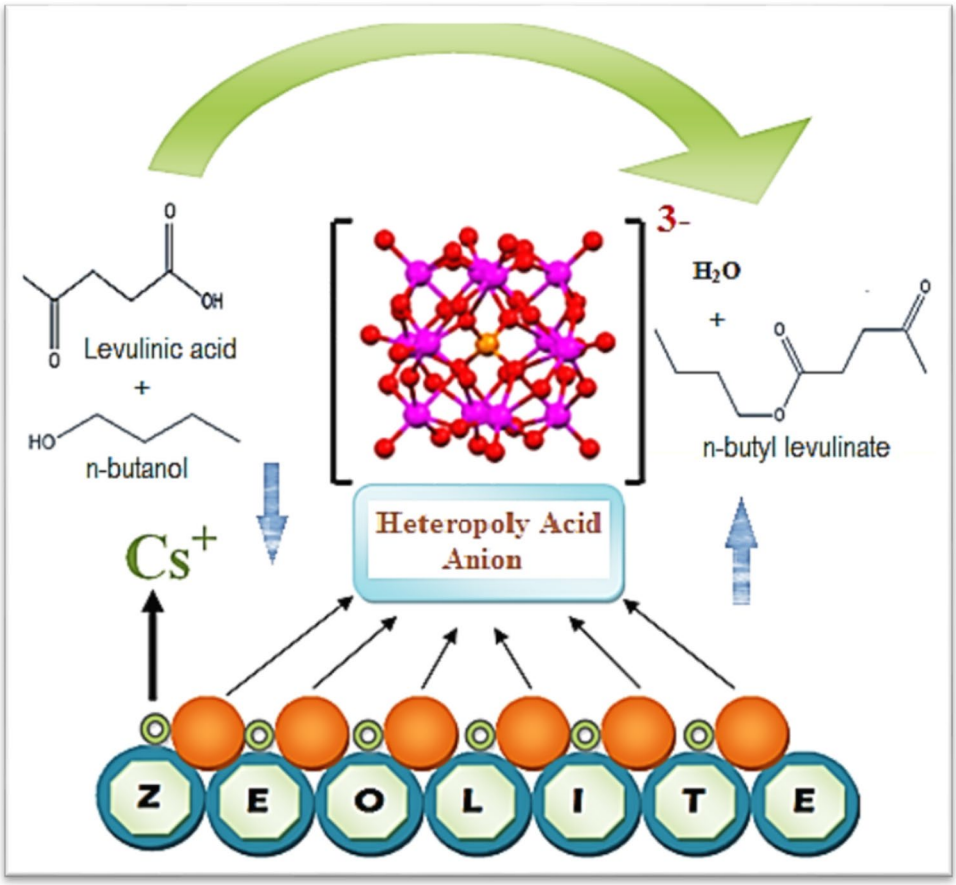

Scheme 1 Cs exchanged TPA supported zeolite catalyzed esterification of levulinic acid

to 20 wt% on zeolite H-Zβ. The excess water was removed by stirring on a hot plate. The catalyst products were dried at 120 °C for overnight and finally calcined at 300 °C for 2 h. The catalyst obtained after calcination is denoted as CsTPA-Zβ and the procedure is given schematically in Fig. 3. Cs supported Zβ (Cs-Zβ) was prepared in the similar manner, without adding TPA, and the Cs content was kept similar to that of the CsTPA-Zβ catalyst. Similarly, 20 wt% TPA supported Zβ (TPA-Zβ) was prepared without adding Cs and labelled as TPA-ZβRT (RT refers to room temperature). Subsequently, this TPA-ZβRT was calcined at different temperatures (300, 400, 500, 600 and 750 °C) and the resultant catalysts are denoted as TPA-Zβ300, TPA-Zβ400, TPA-Zβ500, TPA-Zβ600, TPA-Zβ750.

2.1.2 Characterization Techniques

Advance D8, Series II Bruker powder X-ray diffractometer with Cu-K_α radiation ($\lambda = 1.5418$ Å), equipped with a nickel filter, was used to determine the phase purity and crystallinity of the synthesized zeolite-based catalysts. The wide-angle scan was made from 2θ value 10º to 80°. Surface area analysis was carried out on Micromeritics adsorption equipment (Model ASAP 2000) at – 196 ºC, using nitrogen. The

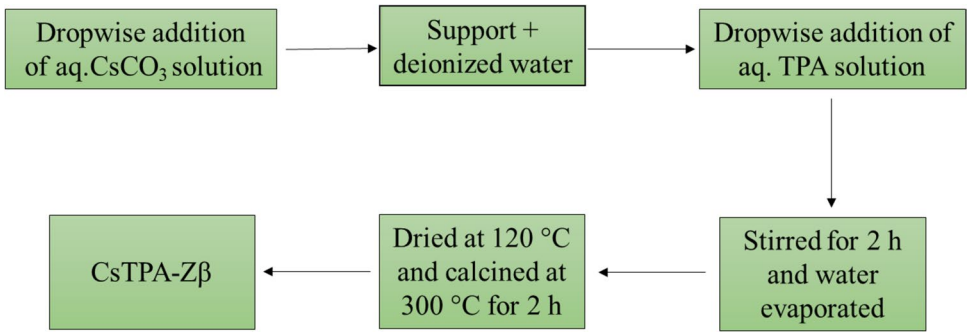

Fig. 3 Synthesis of Cs salt of TPA supported on Zβ (CsTPA-Zβ) catalyst

surface area of the catalysts was determined using the data obtained from the nitrogen sorption isotherms employing the Brunauer–Emmett–Teller (BET) method. The pore volume analysis was carried out using the Barrett-Joyner-Halenda (BJH) method. The elemental analysis was carried out based on SEM-EDAX measurements using JEOL Make microscope (Model JSM 6010) and the images and data are provided as supplementary information (Fig. S1). The acidity of the catalysts was investigated using Quantachrome (USA) Make instrument by NH_3-TPD method. For this purpose, the sample was subjected to ammonia adsorption at 120 ºC and then desorption was carried out to 700 ºC, at a heating rate of 10 ºC/min. TPD profiles are provided in supplementary information (Fig. S2). The ATR-FTIR spectrum of the catalyst were obtained using Perkin Elmer FT-IR spectrum GX. FT-IR spectrum of selected samples was recorded using a pellet prepared by mixing 200 mg of KBr and 0.3 mg of catalyst sample.

2.1.3 Typical Procedure for the Esterification of LA with *n*-Butanol

The esterification reaction was carried out with the calcined catalysts using the methods reported in earlier work [2]. Typically, the esterification of LA was performed in a round bottom (RB) flask connected to a condenser, equipped with a magnetic stirrer in an oil bath. Initially, the 50 mL RB-flask was charged with *n*-butanol, LA and the desired amount of preactivated catalyst. Afterwards, the system was heated to a specific temperature of 120 °C, and the reaction was performed for a specific period of time. The crude products were recovered by evaporating the solvent under reduced pressure and recrystallized with ethanol to get pure *n*-butyl levulinate. The yield of the product formed was estimated by titration with 0.1 M KOH-EtOH solution. The ester yield was calculated using the following equation [20]:

$$\% \text{ Yield } = [(A_i - A_t)/A_i] \times M \times 100,$$

where, A_i = Initial acid value of the reaction mixture (i.e., before reaction), A_t = Acid value of reaction mixture at time 't', M = Mole ratio of LA: alcohol.

The yield of the product formed was also determined using a gas chromatogram (GC) (Agilent-7890 A, equipped with a capillary column, HP-5, 30 m × 0.32 mm × 0.25 µm) with Helium gas as the carrier. Ethanol was used to wash the catalyst and subsequently dried overnight at 60 °C and subsequently reactivated by air at a specific temperature for 4 h before being used to investigate the recyclability of the catalysts. The product, *n*-butyl levulinate, was characterized by comparing its physical data with the known compound [22] and spectral data.

3 Results and Discussion

3.1 XRD

The XRD patterns of the TPA-Zβ samples calcined at 300, 400, 500, 600 and 750 °C are shown in Fig. 4. It can be observed that TPA-Zβ catalysts treated between RT and 400 °C show a similar pattern to that of Zβ. No characteristic peak for TPA was observed, indicating that the active component (TPA) is highly dispersed and also possibly present as poorly crystalline on the Zβ support. However, increasing the calcination temperature beyond 400 °C leads to the decomposition of the Keggin ion of TPA. This is clearly evident from the observed three additional peaks (in the magnified portion between 2θ values of 15 º and 30 º, as shown on the right side, in the Fig. 4).

Specifically, additional peaks are observed in the range of 2θ value from 22.5 to 25° for the catalysts calcined in the range of 500–750 °C, indicating the formation of the WO_3 phase in these catalysts [24, 25]. This is in agreement with the XRD pattern of WO_3 reported by Jagadeeswaraiah et al. [26]. However, the XRD reflections corresponding to Zβ support remained unchanged when the calcination temperature was increased to 750 °C. These results suggest that TPA on Zβ support is thermally stable up to 400 °C. In the case of CsTPA-Zβ and Cs-Zβ samples calcined at 300 °C, the Keggin structure is preserved (pl. refer Fig. 5). No peaks related to caesium oxide were observed. This indicates that CsTPA is highly dispersed on zeolite support. In general, CsTPA shows a characteristic peak at 2θ of *ca* 10º [17] and a similar peak is also observed in the CsTPA-Zβ catalyst, calcined at 300 °C. These results indicate that the Keggin structure of CsTPA remains intact on the Zβ support. (Fig. 5). This result is in line with the literature [27].

3.2 Nitrogen Physisorption Analysis

The results of N_2 sorption isotherms analysis as well as pore size distribution (see inset) of the catalysts are shown in Fig. 6. The BET surface area and pore volume along with ammonia uptake values of the catalysts are given in Table 1. The parent Zβ exhibited Type IV sorption isotherms [Fig. 6(A4)] [28].

A similar pattern is observed for Cs-TPA-Zβ, TPA-Zβ and Cs-Zβ catalysts. This reveals the absence of any structural changes in the zeolite framework due to impregnation of CsTPA, TPA and Cs etc. This is also evidenced by XRD analysis (vide supra). Impregnation of Cs on Zβ resulted in a low BET surface area (599 cm^2/g) (BET surface area of Zβ is 677 cm^2/g) and pore volume (0.76 cc g^{-1}), which was due to

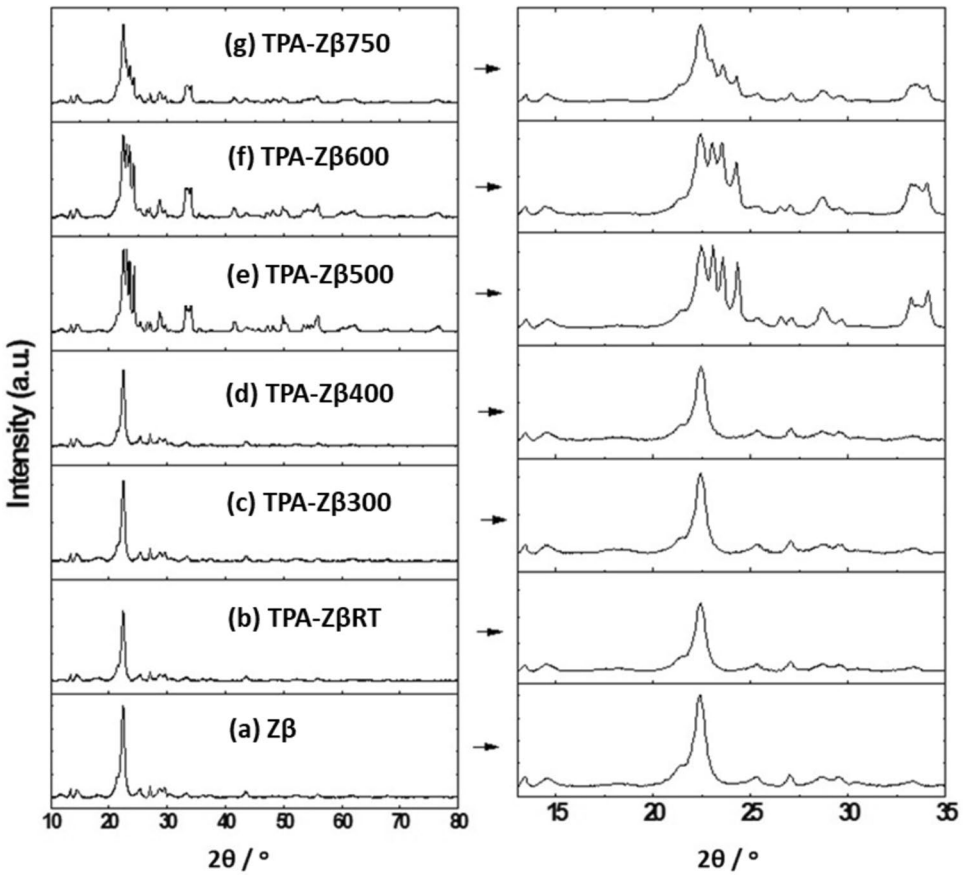

Fig. 4 X-ray diffraction patterns of TPA-Zβ catalysts calcined at different temperatures: (**a**) Zβ, (**b**) TPA-ZβRT, (**c**) TPA-Zβ300, (**d**) TPA-Zβ400, (**e**) TPA-Zβ500, (**f**) TPA-Zβ600, and (**h**) TPA-Zβ750. On the right, magnified range of the XRD pattern in the specific region is given

the blocking of some zeolite pores by Cs^+ ions, as observed by the low pore volume. In the case of TPA-Zβ, the BET surface area is reduced to 498 cm^2/g. The pore volume also follows the same trend due to the presence of larger Keggin ions in the TPA-Zβ catalyst. Whereas, CsTPA-Zβ exhibited a moderate BET surface area of 574 cm^2/g (between the surface areas of Cs-Zβ and TPA-Zβ). The higher surface area of CsTPA-Zβ than TPA-Zβ catalyst can be explained as follows: Heteropoly tungstate exhibits low surface area (< 10 m^2/g) and when Cs^+ ions are incorporated into the secondary structure of the Keggin ion, enhancement of the surface area is generally observed [29]. A similar trend is observed for TPA and CsTPA supported on Zβ and other supported catalysts [30]. No significant difference was found between the pore volume and pore diameters of TPA-Zβ and CsTPA-Zβ catalysts. The ammonia TPD profiles of Zβ, TPA-Zβ and CsTPA-Zβ catalysts are presented in the supplementary information (Fig. S1). Pure Zβ exhibited a strong desorption peak in the range of 120–550 °C with a shoulder around at 350 °C (related to moderate acidic sites). The total amount of ammonia desorbed in pure Zβ was found to be 1.21 mmol g^{-1}. For the TPA-Zβ and CsTPA-Zβ catalysts, the desorption peaks were similar to those of the starting zeolite. However, the shoulder peak disappeared (merged with the main peak) in both catalysts, indicating a strong interaction between the Keggin primary units of heteropoly acid with zeolite. Since it is known that zeolites and HPAs are known for Bronsted acidity i.e., the main contributor to the acidity is the presence of protons. The total desorbed ammonia for TPA-Zβ and CsTPA-Zβ catalysts is 0.88 and 0.59 mmol g^{-1},

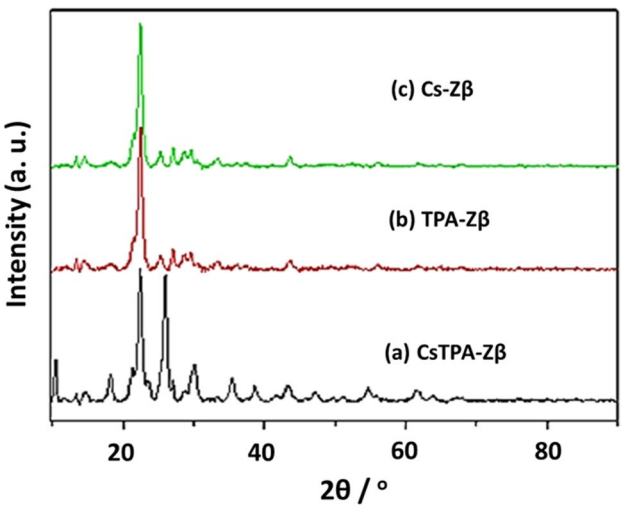

Fig. 5 XRD patterns of (**a**) CsTPA-Zβ, (**b**) TPA-Zβ, and (**c**) Cs-Zβ catalysts

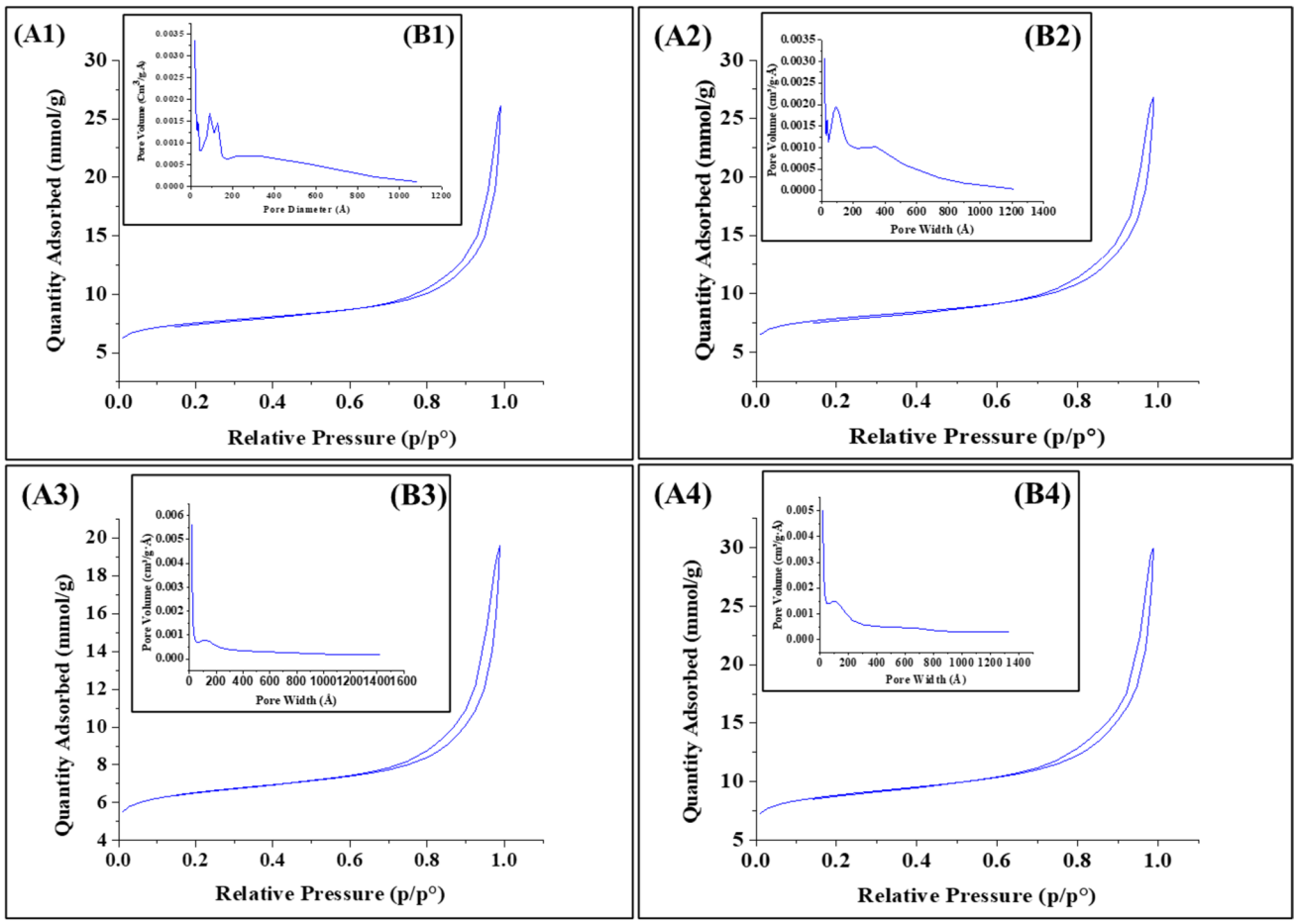

Fig. 6 N_2 adsorption–desorption isotherms of CsTPA-Zβ (A1), Cs-Zβ (A2), TPA-Zβ (A3), parent Zβ (A4) and pore size distribution (inset) of CsTPA-Zβ (B1), Cs-Zβ (B2), TPA-Zβ (B3), parent Zβ (B4)

Table 1 BET surface area, pore volume and acidity data of the catalysts

Catalyst type	BET surface area (cm^2/g)[a]	Pore vol. (cm^3/g)	Pore diameter (nm)[b]	Ammonia uptake (mmol/g)[c]
Zβ	677	0.84	4.35	1.21 (at 219 °C, weak and moderate)
TPA-Zβ	498	0.63	4.37	0.88 (at 199 °C, weak and moderate)
CsTPA-Zβ	574	0.74	4.57	0.59 (at 213 °C, weak)
Cs-Zβ	599	0.76	4.39	–

[a]BET method

[b]BJH method

[c]NH_3-TPD method

respectively. A minor decrease in the total acidity of the TPA-Zβ catalyst compared to the parent Zβ might be due to the presence of shared protons between the zeolite surface and the Keggin ion (no shoulder peak was observed i.e., strong interactions). Therefore, the acidity of TPA-Zβ acidity comes from the shared protons. In contrast, in the case of Zβ, the free protons on the zeolite surface are the main contributor to the acidity. In the case of the CsTPA-Zβ catalyst, the total acidity decreased further (0.59 mmol g^{-1}) and is due to the presence of Cs^+ ions (which were replaced protons). Thus, it can be said that the residual protons shared between the zeolite and the Keggin unit contribute to the acidity of the CsTPA-Zβ catalyst. SEM–EDX images of Cs-Zβ, TPA-Zβ, and CsTPA-Zβ catalysts are presented in Fig. S2. All catalysts presented the presence of the respective elements used for their preparation.

3.3 FT-IR and ATR FT-IR Spectral Studies

FT-IR spectroscopy is a powerful tool not only for characterizing organic molecules, but also it gives valuable information about inorganic compounds. The existence of the Keggin structure of HPAs in the synthesized catalysts is confirmed by ATR-FT-IR spectroscopy. The IR spectra of parent zeolite Zβ and synthesized Cs-Zβ, TPA-Zβ, and CsTPA-Zβ catalysts are depicted in Fig. 7.

The ATR-FT-IR spectrum of the CsTPA-Zβ sample exhibited characteristic bands in the range of 1100–500 cm^{-1} (fingerprint region) of HPA. The peak observed at 1067 cm^{-1} is related to the P–O stretching vibration of the central PO_4 ion. Three additional bands at 988, 889, and 806 cm^{-1} are ascribed to W = O_t (O_t = terminal oxygen) asymmetric stretching, asymmetric stretching in W-O_c-W (O_c = corner-sharing bridging oxygen), and the asymmetric stretching in W–O_e–W (O_e = edge-sharing bridging oxygen atom), respectively [21, 31]. The band observed at 806 cm^{-1} corresponds to v_{as} (W–O–W) for the Keggin-type polytungstate ion, $[PW_{12}O_{40}]^{-3}$. Further, the v_{as} (P–O) band split into two bands and the band attributed to v_{as} (W–O–W) was split into multiple bands due to change in symmetry of the heteropoly anion from T_d to C_s. The band observed at 513 cm^{-1} is also due to O–P–O bending. These bands are observed for the CsTPA-Zβ and some bands are merged with the zeolite bands, indicating that the Keggin ion structure is unaltered after supporting on zeolite. ATR-FTIR spectrum of Zβ (Fig. 7b) shows a broad and large band in the range 1060–1090 cm^{-1}, corresponding to the asymmetric stretching of the external linkages [v_{as} (O–T–O)], which is quite sensitive to the Si and Al of Zβ. The band observed at 1273 cm^{-1} is assigned to the asymmetric stretching of internal tetrahedra [32–34].

ATR-FT-IR spectra of all samples (Fig. 7b) exhibited bands at 794 cm^{-1} corresponding to the double ring of the zeolite and symmetric stretching vibrations of SiO_4 and AlO_4. Bands at 564 cm^{-1} is assigned to the 5- and 6-membered rings in the zeolite structure. The band observed at 478 cm^{-1} is assigned to O–T–O (T = Si, Al) bending modes. This band was identified as a characteristic band corresponding to the pore opening of zeolite Hβ. The FT-IR spectra of all samples (Fig. 7a) showed a broad band in the range 3700–3000 cm^{-1} which attributed to the –OH stretching vibrations of the internal silanol groups and the surface silanol groups. The central band observed at 3628 cm^{-1} corresponds to the surface acidic Al–OH groups. The –OH bending vibrations of the water molecules are observed at 1631 cm^{-1} [35].

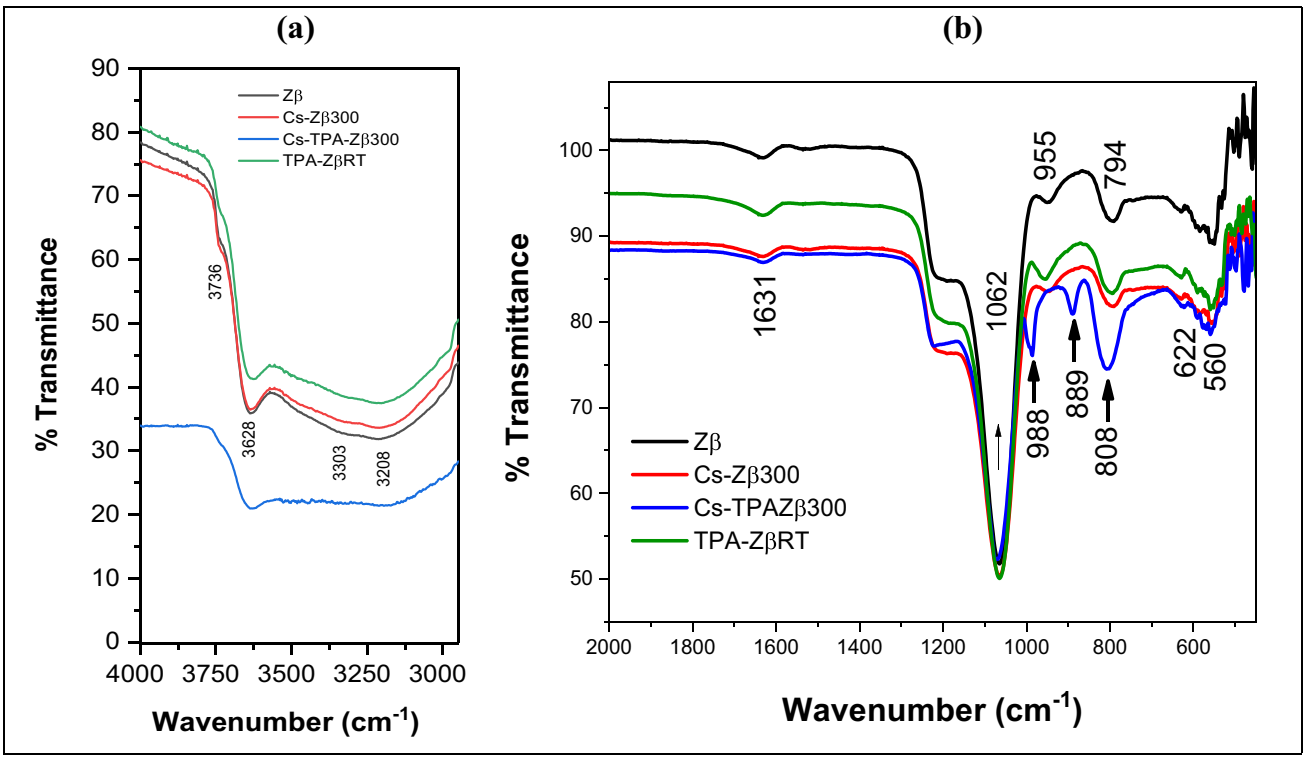

Fig. 7 FT-IR spectra (**a**) of parent zeolite Zβ, CsTPA-Zβ (calcined at 300 °C), Cs-Zβ300 and TPA-ZβRT catalysts. For clarity we show a region of interest. On the left, the FT-IR spectrum region between 4000 and 3000 cm^{-1} represents the hydroxyl region and, on the right, the ATR-FT-IR spectra (**b**) region between, 2000–400 cm^{-1}, showing the zeolite ring and TPA structure vibrations

3.4 Catalytic Activity

The catalytic activity results of the synthesized catalysts for the esterification of LA are discussed in the subsequent sections. All experiments were repeated twice and the errors between the two measurements were within ± 5%.

3.4.1 Effects of Time and Calcination Temperature on Catalytic Activity

The catalytic evaluation of the TPA-Zβ catalyst calcined at various temperatures is studied. Table 2 shows the activity results of the TPAZβ catalyst treated in the range of 300–750 °C along with pure Zβ. The results are also shown in Fig. 8. In the case of parent Zβ, the conversion of LA is 82% after 4 h of reaction time. However, the TPAZβ catalyst calcined at 300 °C showed higher conversion (95.2%) within 2.5 h reaction time. Further increase in the reaction time to 4 h there is no significant change in the conversion was observed, but after 3 h a slight decrease in the conversion of LA was observed this might be due to the presence of water accelerating the reversible reaction as reported by Zhao et al. [36]. When the calcination temperature of the catalyst was increased to 400 °C, the conversion decreased to 89.2%. This could be due to partial degradation of the Keggin heteropoly tungstate at 400 °C. When the calcination temperature was further increased to 500–750 °C, the conversion of LA decreased drastically and was only in the range of 24.8–29.4%. This can be attributed to the complete decomposition of the Keggin ion and the formation of the WO_3 phase on the zeolite surface. This was confirmed by the XRD patterns of the catalyst calcined in the range of 300–750 °C (see Fig. 3). The data reveal that the optimum reaction time in the case of the TPA-Zβ catalyst calcined at 300 °C is 2.5 h. However, the activity of the recycled TPA-Zβ catalyst was (calcined at 300 °C) found to decrease slightly (85%).

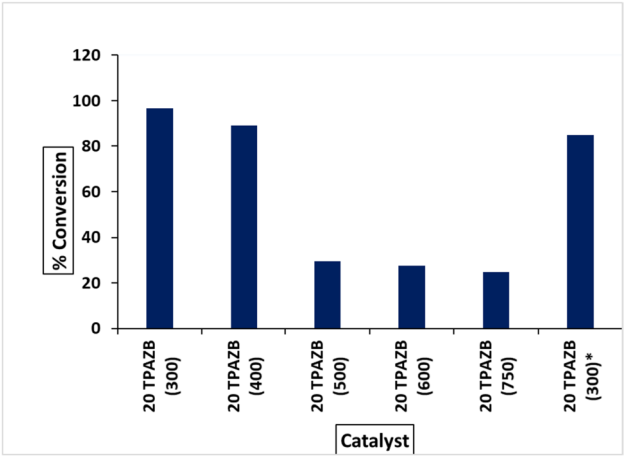

Fig. 8 Effect of calcination temperature on % LA conversion after 2.5 h

3.4.2 Comparative Study and Catalyst Reusability

To improve the catalyst reusability, TPA was partially exchanged with the larger cation Cs^+ and then the LA esterification reaction was performed. The reaction conditions, % LA conversion and yield of *n*-butyl levulinate are shown in Table 3.

The Cs-Zβ catalyst exhibited low activity (61.9% conversion) compared to parent Zβ and other synthesized catalysts. This was due to the exchange of protons of zeolite by Cs^+ ions, resulting in low acidity and activity. The maximum % LA conversion (97.6%) and 88.4% yield of *n*-butyl levulinate was observed in the case of CsTPA-Zβ catalyst within 4 h. While in the case of TPA-Zβ, the maximum conversion was 95.3% within 2.5 h (86.3% yield) (Table 1). The activity of TPA and the Cs salt of TPA

Table 2 Influence of calcination temperature and reaction time of TPA-Zβ catalyst on % LA conversion

Catalysts	Time (h)	% Conversion[a]
H-Zβ	4.0	82.1
TPA-Zβ (300 °C)	4.0	95.3
TPA-Zβ (300 °C)	3.0	90.3
TPA-Zβ (300 °C)	2.5	95.2
TPA-Zβ (400 °C)	2.5	89.2
TPA-Zβ (500 °C)	2.5	29.4
TPA-Zβ (600 °C)	2.5	27.6
TPA-Zβ (750 °C)	2.5	24.8
TPA-Zβ (300 °C)[b]	2.5	85.0

[a]Reaction conditions: LA:*n*-butanol:Catalysts ratio:1:7:10 wt.%; Reaction temperature:120 °C

[b](Recycled)

Table 3 Comparison of catalytic activity of synthesized catalysts towards the synthesis of *n*-butyl levulinate

Catalysts	Time (h)	% LA conversion[a]	% Yield of *n*-butyl levulinate
H-Zβ	4.0	82.1	74.3
TPA-Zβ (300 °C, Fresh)	4.0	95.3	86.3
TPA-Zβ (300 °C, Recycled)	4.0	85.0	77.0
CsTPA-Zβ (300 °C, Fresh)	4.0	97.6	88.4
CsTPA-Zβ (300 oC, Recycled)	4.0	95.8	86.7
Cs-Zβ	4.0	61.9	56.0

[a]Reaction conditions: LA:*n*-butanol:catalyst ratio: 1:7:10 wt. %; Reaction temperature: 120 °C

supported on Zβ catalyst was found higher than that of zeolite Zβ (82.1% within 4 h) and Cs-Zβ (61.91 within 4 h). Further, the TPA-Zβ catalyst (without Cs^+) exhibited a decrease in catalytic activity during the 2nd run (85.0%) compared to CsTPA-Zβ (95.8%). This might be due to the leaching of TPA in the TPA-Zβ catalyst. The Cs salt of TPA is insoluble in polar solvents and the activity of the catalyst remains the same without a marginal decrease in activity. Thus, the incorporation of Cs into TPA-Zβ leads to an improvement in catalyst performance, which can be attributed to the intermediate surface area and suitable acidity of CsTPA-Zβ compared to the parent Zβ and TPA-Zβ catalysts (Table 2). The CsTPA-Zβ catalyst exhibited high activity despite having low acidity, which can be attributed to the high mobility of residual protons as reported in the literature [37].

For the reusability study, the CsTPA-Zβ catalyst was separated by simple filtration after 4 h reaction, washed at least three times with ethanol, and then dried in an oven at 120 °C and then used for the esterification reaction with a fresh reaction mixture. Further, the catalyst was recycled for four successive runs without significant loss of activity (Fig. 9), indicating the efficiency of the catalyst. For the 1st, 2nd, 3rd and 4th catalytic runs, the corresponding % LA conversion and *n*-butyl levulinate % yields are as follows: % LA conversion: 97.6%, 95.8% 94.6% and 94.6% and *n*-butyl levulinate % yield: 88.36%, 86.73%, 85.63% and 85.63%. (Fig. 9). The high activity of the recycled catalyst is due to the super acidity of CsTPA and the acidity of the zeolite support. Thus, the catalyst can be reused.

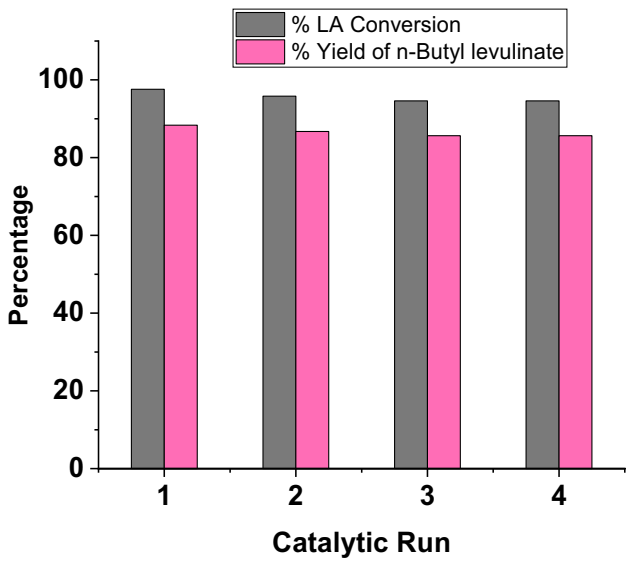

Fig. 9 Catalyst recyclability study. Reaction conditions: LA:*n*-butanol:catalysts ratio: 1:7:10 wt. %; Reaction temperature: 120 °C

4 Conclusion

An eco-friendly method was investigated for the esterification of LA with *n*-butyl alcohol. For the esterification reaction, TPA–Zβ with a calcination temperature of 300 °C was found to be optimal among all other TPA-Zβ catalysts. The activity of the catalysts depends on the intact Keggin ion structure which in turn depends on the catalyst calcination temperature. XRD patterns showed that the Keggin structure of TPA is stable up to the calcination temperature of 300 °C beyond which formation of WO_3 was observed due to decomposition of TPA. The role of Cs was investigated by comparing the activity of TPA-Zβ and CsTPA-Zβ catalysts. A higher catalytic activity was observed for CsTPA-Zβ than for TPA-Zβ (without Cs^+). The acidity of the residual protons plays an important role in the esterification of *n*-butyl levulinate. The residual protons shared between the zeolite and the Keggin unit are responsible for high activity of the CsTPA-Zβ catalyst. The CsTPA-Zβ catalyst was found to be the most efficient and reusable in the synthesis of *n*-butyl levulinate via LA esterification. Thus, the results clearly suggest that Cs containing TPA-Zβ efficiently promotes the catalytic process and moreover, the addition of Cs ions with TPA seems to improve the catalytic performance of zeolite β catalyst.

Supplementary Information The online version contains supplementary material available at https://doi.org/10.1007/s10563-023-09410-1.

Acknowledgements Authors thank Canadian Research Chair Program, NSERC, for financial support. Authors would also like to thank Sud-Chemie India Private Limited, Vadodara for supplying the zeolites samples. RKC thank Slovenian Research Agency (ARRS) for the financial support in the form of project grants, N2-0204 and N1-0261.

Author contributions Dr. Kalpana Maheria - Conceptualization, performed the research work, wrote the main manuscript text, prepared the figures; Prof. (Dr.) Ajay K. Dalai- Contributed in terms of research facility, analysis and reviewed the manuscript; Prof. (Dr.) Janusz Kozinski- reviewed the manuscript, instrumental in providing research facility and analysis support; Dr. Ramesh Chowdari- Contributed in writing characterization and introduction portion pertaining to Heteropoly acids, Reviewed the manuscript

Declarations

Competing interests The authors declare no competing interests.

References

1. Bozell JJ, Petersen GR (2010) Technology development for the production of biobased products from biorefinery carbohydrates—the US Department of Energy's "Top 10" revisited. Green chem 12:539–554. https://doi.org/10.1039/B922014C

2. Maheria KC, Kozinski J, Dalai A (2013) Esterification of levulinic acid to *n*-butyl levulinate over various acidic zeolites. Catal lett 143:1220–1225. https://doi.org/10.1007/s10562-013-1041-3
3. Wu M, Yao X, Jiang J, Ji Y, Gu Y, Deng Q, Ouyang J (2022) Synthesis of magnetic sulfonated carbon/Fe_3O_4/palygorskite composites and application as a solid acid catalyst. Clays Clay Miner 70:514–526. https://doi.org/10.1007/s42860-022-00199-0
4. Morawala DH, Lathiya DR, Dalai AK, Maheria KC (2020) TTAB mediated synthesis of Meso-H-BEA and its application in the production of *n*-butyl levulinate. Catalyst 348:177–186. https://doi.org/10.1007/s10562-019-03005-0
5. Nandiwale KY, Bokade VV (2015) Esterification of renewable levulinic acid to *n*-butyl levulinate over modified H-ZSM-5. Chem Eng Technol 38:246–252. https://doi.org/10.11113/jt.v79.8095
6. Adeleye AT, Louis H, Akakuru OU, Joseph I, Enudi OC, Michael DP (2019) A review on the conversion of levulinic acid and its esters to various useful chemicals. AIMS Energy 7:165–185. https://doi.org/10.3934/energy.2019.2.165
7. Patel A, Joshi M, Sharma S (2022) Designing of a novel heterogeneous catalyst comprising 12-tungstophosphoric acid and zeolite HY for the synthesis of bio-based esters. Biomass Convers Biorefin 13:1–9. https://doi.org/10.1007/s13399-022-03279-2
8. ČejkaJiří Morris RE, Nachtigall P (2017) Zeolites in catalysis: properties and applications. Royal Society of Chemistry, UK. https://doi.org/10.1039/9781788010610
9. Martínez-Iñesta MM, Peral I, Proffen T, Lobo RF (2005) A pair distribution function analysis of zeolite beta. Microporous Mesoporous Mater 77:55–66. https://doi.org/10.1016/j.micromeso.2004.07.040
10. Ohsuna T, Liu Z, Terasaki O, Hiraga K, Camblor MA (2002) Framework determination of a polytype of zeolite beta by using electron crystallography. J Phys Chem B 106:5673–5678. https://doi.org/10.1021/jp0130463
11. Maheria KC, Lodhi A, Sharma G (2021) Microalgae oil upgrading over zeolite-based catalysts. In catalytic and noncatalytic upgrading of oils. ACS Symposium Series, 1379:89–124. https://doi.org/10.1021/bk-2021-1379.ch004
12. Drago RS, Dias JA, Maier TO (1997) An acidity scale for Brönsted acids including $H_3PW_{12}O_{40}$. J Am Chem Soc 119:7702–7710. https://doi.org/10.1021/ja9639123
13. Baroi C, Dalai AK (2014) Review on biodiesel production from various feedstocks using 12-tungstophosphoric acid (TPA) as a solid acid catalyst precursor. Ind Eng Chem Res 53:18611–18624. https://doi.org/10.1021/ie5010866
14. Dias JA, Dias SC, Kob NE (2001) Dehydration of 1-propanol using $H_3PW_{12}O_{40}$ as catalyst. J Chem Soc Dalton Trans 3:228–231. https://doi.org/10.1039/B005256F
15. Tsigdinos GA (2006) Heteropoly compounds of molybdenum and tungsten. Topics in current chemistry: aspects of molybdenum and related chemistry. Springer, Berlin, pp 1–64. https://doi.org/10.1007/BFb0047026
16. Heravi MM, Fard MV, Faghihi Z (2013) Heteropoly acids-catalyzed organic reactions in water: doubly green reactions. Green Chem Lett Rev 6:282–300. https://doi.org/10.1080/17518253.2013.846415
17. Kumar CR, Rambabu N, Maheria KC, Dalai AK, Lingaiah N (2014) Iron exchanged tungstophosphoric acid supported on activated carbon derived from pinecone biomass: evaluation of catalysts efficiency for liquid phase benzylation of anisole with benzyl alcohol. Appl Catal A General 485:74–83. https://doi.org/10.1016/j.apcata.2014.07.034
18. Kuwahara Y, Kango H, Yamashita H (2017) Catalytic transfer hydrogenation of biomass-derived levulinic acid and its esters to γ-valerolactone over sulfonic acid-functionalized UiO-66. ACS Sustain Chem Eng 5:1141–1152. https://doi.org/10.1021/acssuschemeng.6b02464
19. Rafiee E, Joshaghani M, Tork F, Fakhri A, Eavani S (2008) Esterification of mandelic acid catalyzed by heteropoly acid. J Mol Catal A Chem 283:1–4. https://doi.org/10.1016/j.molcata.2007.11.029
20. Chu W, Yang X, Ye X, Wu Y (1996) Vapor phase esterification catalyzed by immobilized dodecatungstosilicic acid (SiW12) on activated carbon. Appl Catal A General 145:125–140. https://doi.org/10.1016/0926-860X(96)00109-3
21. Das J, Parida KM (2007) Heteropoly acid intercalated Zn/Al HTlc as efficient catalyst for esterification of acetic acid using *n*-butanol. J Mol Catal A Chem 264:248–254. https://doi.org/10.1016/j.molcata.2006.09.033
22. Mukai SR, Shimoda M, Lin L, Tamon H, Masuda T (2003) Improvement of the preparation method of "ship-in-the-bottle" type 12-molybdophosphoric acid encaged Y-type zeolite catalysts. Appl Catal A General 256:107–113. https://doi.org/10.1016/S0926-860X(03)00392-2
23. Dharne S, Bokade VV (2011) Esterification of levulinic acid to *n*-butyl levulinate over heteropolyacid supported on acid-treated clay. J Nat Gas Chem 20:18–24. https://doi.org/10.1016/S1003-9953(10)60147-8
24. Patel PP, Morawala DH, Lodhi A, Parmar HS, Maheria KC (2021) H-ZSM-5 catalyzed esterification of levulinic acid to synthesize *n*-pentyl levulinate. Catal Green Chem Eng 4(2):23–33. https://doi.org/10.1615/CatalGreenChemEng.2021037893
25. Lopez-Salinas E, Hernandez-Cortez JG, Schifter I, Torres-Garcıa E, Navarrete J, Gutierrez-Carrillo A, Lopez T, Lottici PP, Bersani D (2000) Thermal stability of 12-tungstophosphoric acid supported on zirconia. Appl Catal A General 193:215–225. https://doi.org/10.1016/S0926-860X(99)00431-7
26. Jagadeeswaraiah K, Ramesh Kumar Ch, Rajashekar A, Srivani A, Lingaiah N (2016) The role of tungsten oxide species supported on titania catalysts for the synthesis of glycerol carbonate from glycerol and urea. Catal Lett 146(3):92–700. https://doi.org/10.1007/s10562-016-1694-9
27. Okuhara T, Watanabe H, Nishimura T, Inumaru K, Misono M (2000) Microstructure of caesium hydrogen salts of 12-tungstophosphoric acid relevant to novel acid catalysis. Chem Mater 12(8):2230–2238. https://doi.org/10.1021/cm9907561
28. Thommes M, Kaneko K, Neimark AV, Olivier JP, Renoso FR, Rouquerol J, Sing KSW (2015) Physisorption of gases, with special reference to the evaluation of surface area and pore size distribution (IUPAC Technical Report). Pure Appl Chem 87(9–10):1051–1069. https://doi.org/10.1515/pac-2014-1117
29. Eom HJ, Lee DW, Kim S, Chung SH, Hur YG, Lee KY (2014) Hydrocracking of extra-heavy oil using Cs-exchanged phosphotungstic acid (CsxH3− xPW12O40, x= 1–3) catalysts. Fuel 126:263–270. https://doi.org/10.1016/j.fuel.2014.02.060
30. Shen H, Zhou Z, Wen G, Xu L, Ding Q, Guan Y, Yang Z, Sun Y, Gao X, Zhang J, Fan X, Jiao Y (2022) Cs exchanged 12-tungstophosphoric acid supported on high-silica mesoporous Y zeolites for synthesis of ethyl lactate via catalytic esterification. Biomass Bioenergy 165:106552. https://doi.org/10.1016/j.biombioe.2022.106552
31. Patel A, Narkhede N (2012) 12-Tungstophosphoric acid anchored to zeolite Hβ: synthesis, characterization, and biodiesel production by esterification of oleic acid with methanol. Energy Fuels 26:6025–6032. https://doi.org/10.1021/ef301126e
32. Fathi S, Sohrabi M, Falamaki C (2014) Improvement of HZSM-5 performance by alkaline treatments: comparative catalytic study in the MTG reactions. Fuel 116:529–537. https://doi.org/10.1016/j.fuel.2013.08.036
33. Kiricsi I, Flego C, Pazzuconi G, Parker WJ, Millini R, Perego C, Bellussi G (1994) Progress toward understanding zeolite beta

acidity: an IR and ^{27}Al NMR spectroscopic study. J Phys Chem 98:4627–4634. https://doi.org/10.1021/j100068a024
34. Ordomsky VV, Murzin VY, Monakhova YV, Zubavichus YV, Knyazeva EE, Nesterenko NS, Ivanova II (2007) Nature, strength and accessibility of acid sites in micro/mesoporous catalysts obtained by recrystallization of zeolite BEA. Microporous Mesoporous Mater 105:101–110. https://doi.org/10.1016/j.micromeso.2007.05.056
35. Labajos FM, Rives V, Ulibarri MA (1992) Effect of hydrothermal and thermal treatments on the physicochemical properties of Mg-Al hydrotalcite-like materials. J Mater Sci 7:1546–1552. https://doi.org/10.1007/BF00542916
36. Zhao W, Ding H, Zhu J, Liu X, Xu Q, Yin D (2020) Esterification of levulinic acid into *n*-butyl levulinate catalyzed by sulfonic acid-functionalized lignin-montmorillonite complex. J Bioresour Bioprod 5:291–299. https://doi.org/10.1016/j.jobab.2020.10.008
37. Chikin AI, Chernyak AV, Jin Z, Naumova YS, Ukshe AE, Smirnova NV, Volkov VI, Dobrovolsky YA (2012) Mobility of protons in 12-phosphotungstic acid and its acid and neutral salts. J Solid State Electrochem 16:2767–2775. https://doi.org/10.1007/s10008-012-1687-6

Authors and Affiliations

Kalpana Maheria[1,2] · Ramesh Kumar Chowdari[2,3] · Janusz Kozinski[4] · Ajay Kumar Dalai[2]

✉ Kalpana Maheria
kcm@chem.svnit.ac.in

✉ Ajay Kumar Dalai
akd393@uskask.ca

Ramesh Kumar Chowdari
chowdarirameshkumar@gmail.com

Janusz Kozinski
jkozinsk@lakeheadu.ca

[1] Department of Chemistry, Sardar Vallabhbhai National Institute of Technology, Ichchhanath, Surat, Gujarat 395007, India

[2] Department of Chemical and Biological Engineering, University of Saskatchewan, Saskatoon, SK S7N 5A9, Canada

[3] Department of Catalysis and Chemical Reaction Engineering, National Institute of Chemistry, 19 Hajdrihova, 1001 Ljubljana, Slovenia

[4] Faculty of Engineering, Lakehead University, 955 Oliver Road, Thunder Bay, ON P7B 5E1, Canada